Gyrokinetic simulations of shaping effects on turbulent heat and particle transport

X. Lapillonne, T. Dannert, O. Sauter, A. Marinoni, Y. Camenen, A. Pochelon, L. Villard and S. Brunner

Ecole Polytechnique Fédérale de Lausanne (EPFL)
Centre de Recherches en Physique des Plasmas, CH-1015 Lausanne (Switzerland)
xavier.lapillonne@epfl.ch

1. Introduction

- Experimental evidence of shaping effects, and especially triangularity, on heat transport coefficient [1, 2] were found on the TCV Tokamak.
- Extention of the gyrokinetic flux tube code GENE [3, 4] from s-alpha approximation to general axisymmetric geometry using an interface with an ideal MHD equilibrium code, CHEASE [5], in order to study the influence of shaping on micro-instabilities.

2. Gyrokinetic equation in general axisymmetric geometry, in the low β limit

Coordinates system

Field aligned coordinates (x, y, z), $x = q_0/(\rho_0 B_0)\Psi, y = \rho_0/q_0(q\chi - \Phi), z = \chi$ where Ψ is the poloidal flux, ϕ is the toroidal angle, and χ is an angle defined in such a way that (Ψ, χ, Φ) is a strait field line coordinate system. q_0 is the safety factor at the considered flux surface, ρ_0 is a normalisation length which corespond to the radius of the flux surface in the circular case and B_0 is a reference magnetic field.

The equations

The distribution function $f(x, y, z, v_\parallel, \mu)$ is split into an equilibrium part f_0 and a perturbed part f_1.

$$\frac{\partial f_1}{\partial t} + \left(\frac{1}{L_N} + \frac{1}{L_T}(v_\parallel^2 + \mu B - 3/2)\right) F_0 \frac{\partial \bar{\Phi}_1}{\partial y} + [\bar{\Phi}_1, f_1] + \frac{1}{B^3}\frac{\mu B + 2v_\parallel^2}{2\sigma_j}\left(K_x\frac{\partial f_1}{\partial x} + K_y\frac{\partial f_1}{\partial y}\right) + \frac{1}{B^3}\frac{\mu B + 2v_\parallel^2}{2}\left(K_x\frac{\partial \bar{\Phi}_1}{\partial x} + K_y\frac{\partial \bar{\Phi}_1}{\partial y}\right) + \alpha_j\frac{v_\parallel}{JB}\frac{\partial F_1}{\partial z} + \alpha_j\sigma_j\frac{F_0 v_\parallel}{JB}\frac{\partial \bar{\Phi}_1}{\partial z} - \frac{\mu\alpha_j}{2JB}\frac{\partial F_1}{\partial v_\parallel}\frac{\partial B}{\partial z} = 0$$

where $\bar{\Phi}_1$ is the gyroaveraged electrostatic potential, $\alpha_j = V_{Tj}/c_s$, $\sigma_j = Z_j T_e/T_j$.
The curvature terms are :

$$K_x = -2(g^{xx}g^{yz} - g^{yx}g^{xz})\frac{\partial B}{\partial z}$$
$$K_y = 2((g^{xx}g^{yy} - (g^{xy})^2)\frac{\partial B}{\partial x} - (L_\perp(g^{xy}g^{yz} - g^{yy}g^{xz}))\frac{\partial B}{\partial z})$$

where the $g^{i,j} = \nabla u^i \cdot \nabla u^j$ are the metric coefficients. J is the Jacobian $J^{-1} = (\nabla x \times \nabla y)\cdot\nabla z$.
The self-consistent electrostatic field is solved using the gyrokinetic Poisson equation :

$$(\tau + 1 - \Gamma_0(b))\Phi_1 = \sum_j \pi B \in J_0(\lambda) g dv_\parallel d\mu$$

with $b = 1/(\tau B^2)\nabla_\perp^2$, $\lambda^2 = 2\mu/B\nabla_\perp^2$ and $\nabla_\perp^2 = g^{xx}\partial^2/\partial x^2 + g^{yy}\partial^2/\partial y^2 + g^{xy}\partial^2/\partial x\partial y$.
note : In the following, simulations are done with one kinetic ion species and adiabatic electrons.

3. Geometry module

Interface with the equilibrium code CHEASE

The CHEASE code is solving the Grad-Shafranov equation, and provides equilibrium quantities on a (Ψ, χ, Φ) grid which are used to compute the geometrical coefficients :

$$g^{xx} = \left(\frac{q_0}{\rho_0 B_0}\right)^2 g^{\Psi\Psi} \;;\; g^{xy} = \frac{1}{B_0}\left(q'\chi g^{\Psi\Psi} + q g^{\Psi\chi}\right)$$
$$g^{yy} = \left(\frac{\rho_0}{q_0}\right)^2 \left((q')^2\chi^2 g^{\Psi\Psi} + 2qq'\chi g^{\Psi\chi} + q^2 g^{\chi\chi} + g^{\phi\phi}\right)$$
$$g^{xz} = \frac{q_0}{\rho_0 B_0} g^{\Psi\chi} \;;\; g^{yz} = \frac{\rho_0}{q_0}\left(q'\chi g^{\Psi\chi} + q g^{\chi\chi}\right) \;;\; g^{zz} = g^{\chi\chi}$$

with $q' = dq/d\Psi$.
The equilibrium is set by providing analytical shape of the last flux surface, current and pressure profiles as input parmeters as well as the value of q at a given position.

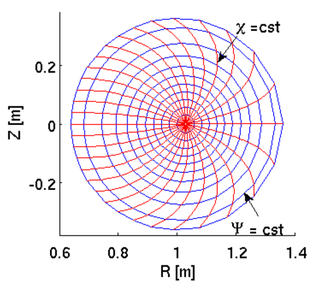

Fig.1 Ψ and χ constant surface

Cyclone case benchmark

Using a circular, low pressure, equilibrium Fig.1, matching the cyclone local parameters at $\rho/a = \sqrt{V/V_{tot}} = 0.5$, namely : $q = 1.4$ and $\rho/qdq/d\rho = 0.78$, simulations are performed for gradients values : $R/L_T = R(d\log T/d\rho)^{-1} = 6.9$, $R/L_N = R(d\log N/d\rho)^{-1} = 2.2$.
Growth rates and real frequencies are compared, Fig. 2, Fig. 3, with simulations using :

- $s - \alpha$ geometry ⇒ growth rate increased by almost a factor 2.
- ad-hoc concentric circular analytic equilibrium, which differs from the $s - \alpha$ model by keeping all terms in $\varepsilon = \rho/R$ ⇒ agreement within 2%
- Flux tube code GS2, using the same equilibrium provided with CHEASE code (EQDSK file) ⇒ agreement within 4%

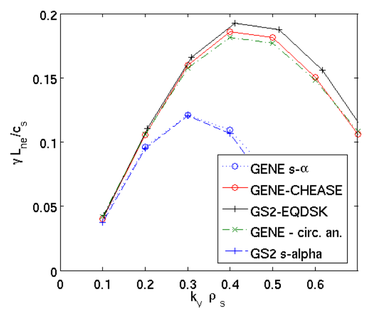

Fig. 2 Growth rate comparisons

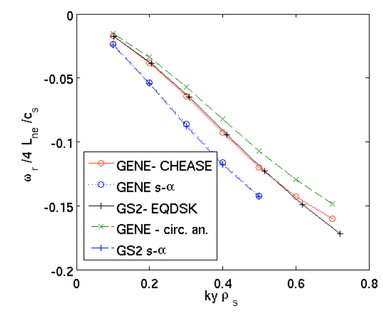

Fig. 3 Real frequencies

The main differences between the general geometry and the $s - \alpha$ model seem to be due to finite aspect ratio contributions neglected in the $s - alpha$ model , this is illustrated by the scan in ε, Fig. 4.

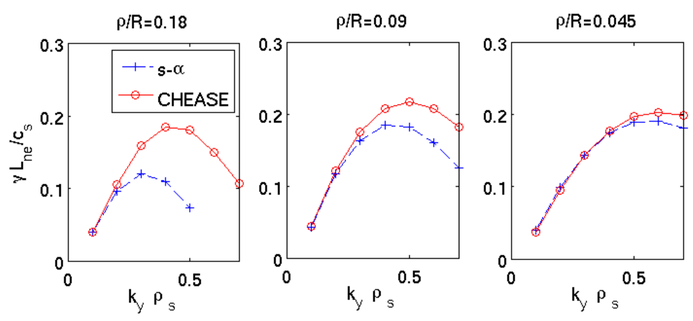

Fig. 4 Growth rate comaprison for different aspect ratio

4. Shaping effects, influence of triangularity

Parameter scan

When changing the geometrical parameters of the last flux surface, two choices are made considering the other equilibrium quantities :

- case A : $< \nabla q >=< \nabla\Psi > dq/d\Psi$, $< \nabla T >$, $< \nabla N >$ are kept constant, where $< \nabla\Psi >$ is the flux surface average of $\nabla\Psi$, referred to as $< \nabla A = \text{cst} >$
- case B : $dq/d\psi$, $dT/d\psi$, $dN/d\psi$ are kept constant, referred to as $dA/d\Psi = \text{cst}$

These quantities are define with respect to there values in the circular cyclone case. In addition q is kept constant for all the following simulations.

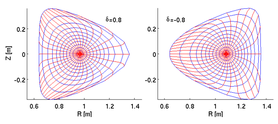
Fig. 5 Plasma with positive and negative triangularity

Linear results

- Fig. 6 : $k_y\rho_s = 0.4$ is the most unstable mode.
- Fig. 7 : The variation of the maximum growth rate is more pronounced when evolving the triangularity at $dA/d\Psi = cst$

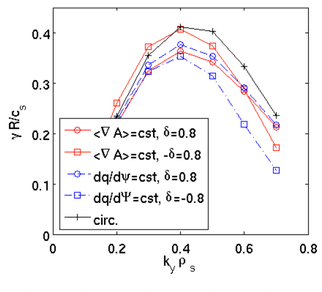

Fig. 6 Growth rate for various triangularities

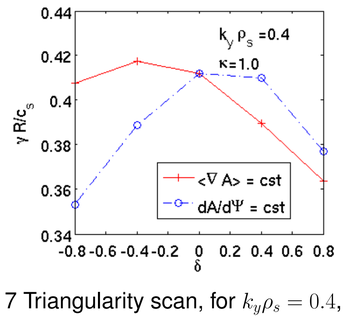

Fig. 7 Triangularity scan, for $k_y\rho_s = 0.4$, $\kappa = 1$

Non-Linear simulations

- Similarly to linear results, low influence of triangularity for $< \nabla A >=$ cst cases.
- 20% decrease of the electrostatic heat flux, for $dq/dpsi =$ cst case and $\delta = -0.8$.

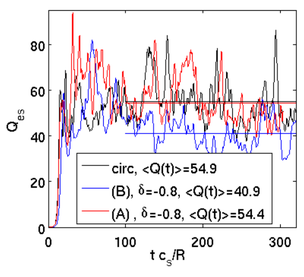

Fig. 8 Time traces of electrostatic heat flux

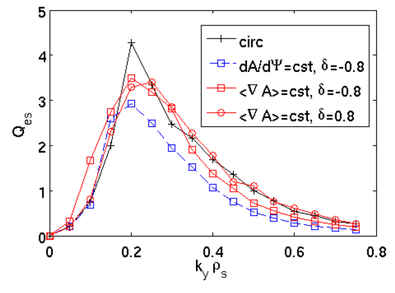

Fig. 9 Electrostatic heat flux spectrum

References

[1] Y. Camenen and A. Pochelon, *et al.*, Plasma Phys. Control. Fusion, **47** (2005) 1971.
[2] Y. Camenen and A. Pochelon, *et al.*, *to be published in Nuclear Fusion*, Impact of plasma triangularity and collisionality on electron heat transport in TCV L-mode plasmas.
[3] F. Jenko, W. Dorland, M. Kotschenreuther, and B.N. Rogers, Phys. Plasmas, **7** (2000) 1904.
[4] T. Dannert and F. Jenko ,Phys. Plasmas , **12** (2005) 1.
[5] H. Lütjens, A. Bondeson, and O. Sauter, Comp. Phys. Com. , **97** (1996) 219.